Appl Microbiol Biotechnol (2017) 101:2397–2413
DOI 10.1007/s00253-016-8020-8

Cyanophycinase CphE from *P. alcaligenes* produced in different compartments of *N. benthamiana* degrades high amounts of cyanophycin in plant extracts

Henrik Nausch[1] · **Inge Broer**[1]

Received: 14 September 2016 / Revised: 17 November 2016 / Accepted: 21 November 2016 / Published online: 9 December 2016

Abstract One of the major constraints in pig and poultry farming is the supply of protein-rich forage, containing sufficient amounts of key amino acids such as arginine (Ufaz and Galili 2008). Since these are underrepresented in plant proteins, the usage of plants as feed is limited. The heterologous production of the cyanobacterial storage polymer cyanophycin granule polypeptide (CGP) in plastids increases the amount of arginine substantially (Huhns et al. 2008; Huhns et al. 2009; Nausch et al. 2016a). CGP degradation releases arginine-aspartate dipeptides. CGP is stable in plants because its degradation is exclusively restricted to bacterial cyanophycinases (CGPases; Law et al. 2009). Since animals are also unable to digest CGP, CGPases need to be co-delivered with CGP-containing plant feed in order to release the dipeptides in the gastrointestinal tract of animals during digestion. Therefore, an extracellular CGPase, CphE from *Pseudomonas alcaligenes* DIP-1, was targeted to the cytosol, ER, and apoplasm of *Nicotiana benthamiana*. Translocation to the chloroplast was not successful. Although CphE accumulated in high amounts in the cytosol, only moderate levels were present in the ER, while the enzyme was nearly undetectable in the apoplasm. This correlates with the higher instability of post-translationally modified CphE in crude plant extracts. In addition, the production in the ER led to an increased number and size of necroses compared with cytosolic expression and might therefore interfere with the endogenous metabolism in the ER. Due to the high and robust enzyme activity, even moderate CphE concentrations were sufficient to degrade CGP in plant extracts.

Keywords Cyanophycinase CphE · *Nicotiana benthamiana* · Protein stability · Post-translational modifications · Enzyme activity

Introduction

Industrial animal fattening, particularly in pig and poultry farming, is predominantly restricted by the provision of protein-rich forage, containing sufficient amounts of semi- and conditionally essential amino acids such as arginine or lysine (FAO 2014; Güttler 2008). This requirement is mainly met by fishmeal which cannot sustainably satisfy the increasing demand in the future. Plants might serve as alternative sources if their content of key amino acids, such as bound arginine and lysine could be increased (Ufaz and Galili 2008). Efforts to achieve this by conventional breeding have so far failed, since their endogenous biosynthesis is regulated by feedback inhibition (Ufaz and Galili 2008). In contrast, crop improvement by genetic engineering has proven more successful, e.g., the lysine content in soy and maize could be significantly raised by introducing regulation-insensitive enzymes of bacterial origin and repressing lysine catabolism in parallel (Ufaz and Galili 2008). Another approach increased the arginine content in tobacco and potato by introducing the

Electronic supplementary material The online version of this article (doi:10.1007/s00253-016-8020-8) contains supplementary material, which is available to authorized users.

✉ Henrik Nausch
henrik.nausch@uni-rostock.de

[1] Faculty of Agricultural and Environmental Sciences, Department of Agrobiotechnology and Risk Assessment for Bio- und Gene Technology, University of Rostock, Justus-von-Liebig Weg 8, 18059 Rostock, VM, Germany

cyanobacterial storage polymer cyanophycin granule polypeptide (CGP) as a sink (Huhns et al. 2008, 2009; Nausch et al. 2016a).

CGP is a polypeptide which naturally occurs in cyanobacterial and non-cyanobacterial prokaryotes, where it serves as a transient store for carbon, nitrogen, and energy (Frommeyer et al. 2014). It is produced by CGP synthetases (CphAs) via non-ribosomal protein biosynthesis, which generates arginine-aspartate dipeptide monomers and links them into a polymer. Subsequently, CGP polymers aggregate and accumulate intracellularly as granules (Law et al. 2009). Apart from arginine, the amino acids lysine, ornithine, and citrulline are incorporated as well as in low amounts (Frommeyer et al. 2014). CGP is resistant to hydrolytic cleavage by common proteases and can only be degraded by dedicated cyanophycinases (CGPases; Law et al. 2009; Sallam and Steinbüchel 2009a). There are two classes of CGPases, CphB and CphE, which both degrade CGP into dipeptide monomers. CphBs are expressed by CGP-producing bacteria and are retained with the cell. In contrast, CphEs are expressed by non-CGP-producing prokaryotes and are secreted in order to utilize CGP from other bacteria. CphE-secreting bacteria were found in the digestive tract of animals as part of the natural microbiota (Sallam and Steinbuchel 2009b). Interestingly, the uptake of dipeptides in the digestive tract of mammals is more efficient compared with free amino acids due to the presence of high-affinity transporters (PEPT1 and PEPT2) in the membrane of the epithelial cells of the small intestine (Broer 2008; Chen et al. 1999; Klang et al. 2005; Lu and Klaassen 2006; Terova et al. 2013). Chemically synthesized dipeptides are already used in industrial animal farming in order to foster the growth and development of livestock that cannot be accomplished by the supply of mere amino acids. They are even used to promote the recovery of human patients (Sallam and Steinbuchel 2010; Santos et al. 2012).

CGP synthesis in plants has been accomplished by the recombinant expression of a cyanobacterial CGP synthetase from *Thermosynecchoccus elongatus* BP-1 ($CphA_{Te}$) in plastids (Huhns et al. 2008, 2009). Tobacco and potato accumulate up to 8.8% and 7.5% of their dry weight (DW) in CGP, respectively (Huhns et al. 2008, 2009; Nausch et al. 2016a). Noteworthy, out of three different CGP synthetases tested, only $CphA_{Te}$ produced CGP in plants (Huhns et al. 2004). This might result from the fact that $CphA_{Te}$ is the only known primer-independent CGP synthetase. A primer seems to be absent in plants (Arai et al. 2004; Nausch et al. 2016b).

Animals should not be able to utilize CGP since (1) they do not possess CGPases, and (2) CGP-degrading bacteria that are present in the gut microbiota are located in the colon (Sallam and Steinbuchel 2009b), while dipeptide absorption takes place in the small intestine (Broer 2008; Sallam and Steinbuchel 2009b), and (3) after addition of CGP to isolates from intestines of several animals, CGP degradation occurred only occasionally (Sallam and Steinbuchel 2009b). Thus, addition of CGPases to CGP-containing feed seems to be required in order to allow dipeptide production and subsequent absorption in the intestine.

Ideally, CGP and CGPases would be co-delivered by the same plant, but CGP and CGPase need to be spatially separated in order to prevent premature CGP degradation (Law et al. 2009). Since CGP is accumulated in plastids, targeting of the CGPase to other compartments seems reasonable to ensure first contact of CGP and CGPase when plant tissue is decomposed during digestion by the animals. However, initial studies, where the CphB-CGPase from *T. elongatus* BP-1 ($CphB_{Te}$) was expressed in the cytosol of tobacco, showed that $CphB_{Te}$ was instable in this compartment and seems to be degraded by endogenous proteases (Ponndorf et al. 2016).

This might be different for a secretory CGPase-like CphE from *Pseudomonas alcaligenes* DIP-1 whose amino acid and DNA sequence (acc. JN620418; Sallam et al. 2011) differ significantly from $CphB_{Te}$. (accession no. P0C8P3; Klemke et al. 2016; Nakamura et al. 2002). In order to analyze the stability of CphE in plants, the enzyme was specifically targeted to the ER, the apolasm, and plastids in addition to its localization in the cytosol.

Materials and methods

Plasmid construction

The plasmid encoding the native coding region (cds) of CphEal (accession no. JN620418), including the Sec secretion signal peptide as described by Sallam et al. (2011), was kindly provided by Cysal GmbH (Münster, Germany). Due to an unintended amino acid substitution at position 241 (glycine (G) to aspartic acid (D)) of the mature protein, which occurred during sub-culturing of the *Escherichia coli* strain without an apparent effect on the enzyme activity (Cysal, personal communication), the sequence and protein are named *cphE241bac* and CphE241 hereafter. The nucleotide sequence was submitted to GenBank under the accession no. KY131983. The cds was amplified without the Sec-leader peptide and the terminal stop codon (Fig. 1a), using the primers *Nco*I-CphEbac-fw and *Xho*I-CphEbac-rv (Table 1). Thereby, restriction sites for *Nco*I and *Xho*I were fused to the 3′ and 5′ end of the cds, respectively. The PCR product was integrated into pJET1.2 (CloneJET PCR Cloning Kit; Thermo Fisher Scientific, Braunschweig, Germany), and subsequently transferred to pET28a (Merck KGaA, Darmstadt, Germany) via *Nco*I/*Xho*I. In the corresponding plasmid pET28a-CphE241bac, the cds was translationally fused to a C-terminal His-tag and a stop codon. The *Xho*I restriction site between the 3′ end of CphE241 and the 5′ end of the His-tag introduced two amino acids leucine (L) and glutamine (E; Fig. S1). *Bsa*I restriction

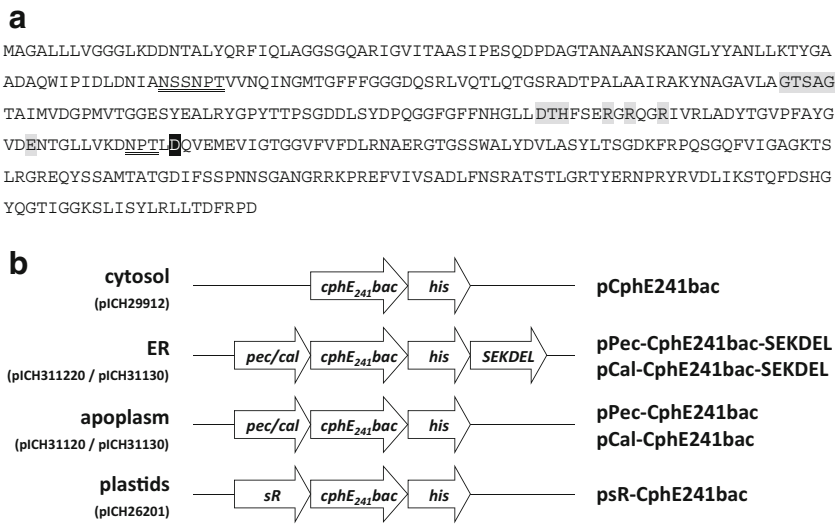

Fig. 1 Constructs used for the transient expression of CphE241 in *N. benthamiana*. **a** Amino acid sequences of mutated CphE241; amino acid substitution is shaded in *black*; amino acids of the catalytic domain are shaded in *gray*; potential *N*-glycosylation sites are *underlined*. **b** Schematic presentation of coding regions, leading to cytosolic, ER-targeted, apoplasm-targeted, and plastid-targeted expressions of CphE241; *cphE241bac* coding region, *his* His-tag, *SEKDEL* ER-retrieval peptide, *pec/cal* ER-targeting peptides, *sR* plastidic transit peptide, *pICH29912, pICH31120, pICH31130,* and *pICH26201* MagnICON vectors

sites were fused 5′ and 3′ to *cphE241bac-his* via the next amplification (primer pair 29-*Bsa*I-cphEbac-fw and 29-*Bsa*I-cphEbac-rv (Table 1)). The PCR product was integrated into pJET1.2 and subsequently transferred either into pICH29912 or pICH26201 for translational fusion with a synthetic (dicotyledonous consensus) transit peptide of the RuBisCO small subunit (sR) to the N-terminal site of CphE241 (Kalthoff et al. 2010), both provided by Nomad BioScience (Halle/Saale, Germany). Targeting to the apoplasm was accomplished by amplification of *cphE241bac-his* from pET28a-CphE241bac (primer pair 31-*Bsa*I-CphEbac-fw/29-*Bsa*I-CphEbac-rv), subcloned through pJET1.2 into pICH31120 and pICH31130,

Table 1 Primer used for the construction of *cphE* encoding MagnICON vectors

Primer	Sequence
*Nco*I-CphEbac-fw	5′-tttttccatggccggagcgctgctgctggtggg-3′
*Xho*I-CphEbac-rv	5′-TTTTTCTCGAGGTCGGGACGGAAGTCGGTCAGC-3′
29-*Bsa*I-CphEbac-fw	5′-tttttGGTCTCACatggccggagcgctgctgctgg-3′
31-*Bsa*I-CphEbac-fw	5′-tttttGGTCTCAAGGTatggccggagcgctgctgctgg-3′
29-*Bsa*I-CphEbac-rv	5′-TTTTTGGTCTCAAAGCTTAGTGGTGGTGGTGGTGGTGCTCGAGG-3′
His-SEKDEL-Oligo	5′-TCGAGCATCATCATCATCATCATTCTGAGAAGGATGAGCTTTAAG CTTACTAGAGCGTGGTGC-3′
	3′-CGTAGTAGTAGTAGTAGTAAGACTCTTCCTACTCGAAATTC GAATGATCTCGCACCACG-5′
29-*Bsa*I-CphEsyn-fw	5′-tttttGGTCTCACATGGCTGGTGCATTACTGTTGGTCGG-3′
29-*Bsa*I-CphEsyn-rv	5′-tttttGGTCTCAAAGCTTAGTGATGATGGTGATGATGCTCC-3′
Actin-fw[a]	5′-GCAACTGGGATGATATGGAGAA-3′
Actin-rv[a]	5′-GTGCCTTTGCAATCCACATCTG-3′
GFP-fw	5′-CACAAGTTCAGCGTGTCCGGCGAGG-3′
GFP-rv	5′-ACCATGTGATCGCGCTTCTCGTTGGG-3′
CphEbac-fw	5′-CTCGACAACATCGCCAACAGCAGCAACC-3′
CphEbac-rv	5′-CATTGCGCAGGTCGAAGACGAATACGCC-3′
CphEsyn-fw	5-CGGTTCTTGCAGGCACCTCTGCTGG-3′
CphEsyn-rv	5′-AGGTTTTCTACGCCCGTTTGCGCC-3′

Restriction sites are solid underlined; His-Tag encoding sequence is dotted underlined; SEKDEL encoding sequence is double underlined

[a] The sequence of the actin primers were taken from Liu et al. (2005), designed for *N. benthamiana*)

leading to a translational fusion to the ER-targeting peptides of the pectinase from *Pyrus malus* (accession no. P48978, pICH31120) and calreticulin from *Nicotiana plumbaginifolia* (accession no. Z71395, pICH31130) to the N-terminus. Both vectors are derivatives of pICH29912 and were provided by Nomad BioScience (Fig. S2). ER retrieval was achieved through addition of a SEKDEL retention signal via substitution of the C-terminal end of the *cphE241bac-his* sequence in these vectors by a His-SEKDEL-encoding Oligo (Table 1), synthesized by Eurofins Genomics GmbH (Ebersberg, Germany), using *Xho*I/*Fsp*AI (Fig. 1b).

GeneOptimizer software from Eurofins Genomics was used to adapt the sequences *cphE241bac* and *cphEal* (accession no. JN620418), to the codon usage of *Nicotiana*, Eurofins Genomics delivered the synthesized fragments *cphE241syn* and *cphEalsyn* in the vector pEX-K4, respectively (Fig. S1). The nucleotide sequences were submitted to GenBank under the accession no. KY131981 and KY131982. After amplification with the primer pair 29-*Bsa*I-CphEsyn-fw/29-*Bsa*I-CphEsyn-rv (Table 1) and sub-cloning into pJET1.2, the fragments were introduced into pICH29912 by *Bsa*I restriction/ligation.

All plasmids were verified by restriction and sequencing (Eurofins Genomics GmbH).

The vector pICH18711, encoding a codon-optimized sequence of cytosolic GFP (Marillonnet et al. 2004), was provided by Nomad BioScience.

The *E. coli* BL21 strain, containing the cyanophycinase $CphB_{Te}$ encoding plasmid pET22b-$CphB_{Te}$, has been kindly provided by Ponndorf et al. (2016).

Overexpression of cyanophycinases in *E. coli* BL21 and preparation of crude extracts

Overexpression of CphE241 and $CphB_{Te}$ was conducted with the plasmids pET28a-CphE241 and pET22b-$CphB_{Te}$ in *E. coli* BL21 using the same protocol. Clones were picked from plates, resuspended in 0.5 ml LB medium and transferred into a 250-ml flask with 50 ml LB, containing 1% glucose and either 100 μg/ml kanamycin (Km) or 125 μg/ml ampicillin (Amp) for the selection of pET28a-CphE and pET22b-$CphB_{Te}$, respectively. After incubation for 2 h at 37 °C and 220 rounds per minute (rpm) in a rotary shaker, cultures were centrifuged in 50-ml reaction tubes (4,566×*g*, 22 °C, 10 min). Pellets were resuspended in 100 ml LB without glucose containing either 100 μg/ml Km or 125 μg/ml Amp and incubated for 2 h at 37 °C. After centrifugation, pellets were resuspended in 200 ml LB without glucose, containing either 100 μg/ml Km or 250 μg/ml Amp, respectively, and 1 mM IPTG for induction of the expression of the target proteins. Cultures were incubated overnight at room temperature (RT; 18–22 °C). The following day, cultures were centrifuged in 50-ml reaction tubes (4,566×*g*; 4 °C; 15 min). The pellets were stored at −28 °C or immediately processed.

For preparation of crude *E. coli* extracts, cell pellets were resuspended in 30 ml ice-cold NPI-lysis buffer (50 mM NaH_2PO_4 (pH = 8.0), 300 mM NaCl, 10 mM imidazol). Cooled in an ice-water mixture, cells were lysed by sonification using the Bandelin Sonotrode HD2200 (BANDELIN electronic GmbH & Co. KG, Berlin, Germany) in combination with the microtip MS73 by applying 3 × 30 s maximal power separated by 1 min break. The cell debris was sedimented by another centrifugation step (4,566×*g*, 4 °C, 15 min) and the supernatant, containing the total soluble protein (TSP), was transferred to a new 50-ml reaction tube. Crude TSP extracts were stored at 4 °C until Ni-NTA purification of His-tagged target proteins.

Plant material and transient expression

For transient expression, vectors were transferred to *Agrobacterium tumefaciens* strain ICF320 (Bendandi et al. 2010). Several bacterial colonies were collected and inoculated into 5 ml LB containing 50 μg/ml rifampicin and 50 μg/ml kanamycin and incubated overnight at 28 °C and 220 rpm in an orbital shaker. Two milliliters of the starter culture were diluted twice in 200 ml LB, containing the same antibiotics, and again incubated at 28 °C/220 rpm overnight in 250-ml flask. The pooled cultures were diluted with LB to an $OD_{600\ nm}$ of 1.5. Subsequently, 500 ml of the adjusted culture were sedimented by centrifugation (4,566×*g*, RT, 15 min) and resuspended in 5 l of infiltration buffer containing 10 mM MES (pH 5.5) and 10 mM $MgCl_2$ (1:10 dilution). One milliliter of the detergent Silwet Gold was added. For vacuum infiltration, 6–9-week-old *Nicotiana benthamiana* plants were submerged upside down into the Agrobacteria suspension and a vacuum of 75–100 mbar was applied for 3 min, using a freeze dryer (Alpha 1-4 Freeze Dryer; Martin Christ Gefriertrocknungsanlagen GmbH, Osterode am Harz / Germany). Infiltrated plants were kept in the dark for one night.

Total soluble protein extraction from leaf tissue and isolation of plastidic protein

In order to prepare crude leaf extract containing the TSP, all leaves per plant were collected and shock-frozen in liquid nitrogen. After grinding on ice, 10 g of leaf material were transferred into a 50 ml Falcon tube and further homogenized in 25 ml of ice-cooled NPI-lysis buffer, using a Polytron PT2100-Homogenizer (30,000 rpm; 30–45 s). The cell debris was sedimented by repeated centrifugation (4,566×*g*, 4 °C, 30 min), and the supernatant transferred into another 50 ml Falcon tube. The protein concentration was determined using Pierce™ Coomassie Plus (Bradford) Assay Kit (Thermo Fisher Scientific, Braunschweig, Germany) according to the manufacturer's instructions.

For isolation of chloroplasts, a protocol was developed on the basis of Fan et al. (2009)—10 g of freshly harvested leaf material were homogenized in approximately 30 ml ice-cold plastid extraction buffer (50 mM HEPES/KOH (pH = 7.8), 300 mM D-Sorbit, 1 mM $MgCl_2 \cdot 6H_2O$, 2 mM EDTA, 0.1% polyvinylpolypyrrolidone (PVP), and 0.04% ß-mercaptoethanol) with mortar and pestle, filtered through Miracloth layers and centrifuged in a 50-ml reaction tube (1500×*g*, 4 °C, 30 min). The supernatant, containing the cytosolic protein fraction, was transferred to another reaction tube and stored at −28 °C for further analysis. The pellet, containing the plastid fraction, was resuspended in 4 ml ice-cold plastid isolation buffer (50 mM HEPES/KOH (pH = 7.8), 300 mM D-Sorbit, 1 mM $MgCl_2 \cdot 6H_2O$, and 2 mM EDTA) and loaded on top of 40 ml of plastid isolation buffer containing 50% sucrose (*w*/*v*). After centrifugation (4,566×*g*, 4 °C, 30 min), intact plastids were collected from the interphase, loaded onto a Percoll step gradient (10%, 30%, and 50% diluted in the plastid isolation buffer) and centrifuged again (8,000×*g*, 4 °C, 20 min). After collection from the interphase between 30% and 50% Percoll, the plastid fraction was divided into 250-μl aliquots, which were resuspended in 1.6 ml of plastid isolation buffer. After centrifugation in 2-ml reaction tubes (16,100×*g*; 4 °C; 15 min), pellets were resuspended in 200 μl ice-cooled NPI-lysis buffer and eight pellets pooled. After another centrifugation, each pooled fraction was resuspended again in 200 μl ice-cold NPI-lysis buffer, pooled, and centrifuged. In this way, the plastid fraction was constricted to a final volume of 1.6 ml and stored at −28 °C until further analysis. Isolation of plastids was confirmed by Western blot analysis of the plastidic protein PsbO.

Western blot analysis

For Western blot analysis, TSP samples were freeze-dried and resuspended in 25 μl loading buffer containing 10% glycerin, 150 mM Tris (pH 6.8), 3% SDS, 1% β-mercaptoethanol, and 2.5% bromophenol blue. After denaturing at 95 °C for 5 min, samples were separated by a 12% SDS-PAGE and electrophoretically transferred to a 0.45-μm Hybond ECL nitrocellulose membrane (GE Healthcare Europe GmbH, Freiburg, Germany), using a BioRad Trans-Blot semi-dry transfer cell. 2 mA/cm^2 were applied for 1 h using 50 mM Tris, 40 mM glycine, 0.01% SDS, and 20% methanol as the transfer buffer (pH 8.5).

In order to detect recombinant CphE with a His-tag specific antibody, membranes were blocked with 20 mM Tris (pH 7.6), 150 mM NaCl, and 0.05% Tween20 (TBSTween20) and 5% nonfat milk powder for 2 h at room temperature. After three washes with TBSTween20, membranes were probed at room temperature (RT) for 2 h with a mouse monoclonal anti-His antibody (cat. no. DIA 900; Dianova, Hamburg Germany) at 1:1,000 dilution in Signal Boost ImmunoReaction Enhancer solution I (cat. no. 407207; Merck KGaA, Darmstadt, Germany). Following another washing step, the membranes were further probed at RT for 1 h with a horseradish peroxidase (HRP)-conjugated donkey anti-mouse antibody (cat. no. 715–035-151; Dianova) at 1:10,000 dilution. Again, three washes were done with TBS without Tween20. The signals were detected by incubation in ECL chemiluminescence reagent (ECL reagent I, 1 M Tris (pH = 8.5); 250 mM luminol, 90 mM p-coumaric acid; ECL reagent II, 1 M Tris (pH 8.5), 30% H_2O_2) and subsequent exposure of membranes to a Kodak Biomax light X-ray film (VWR; Darmstadt, Germany) for 1 min.

For the detection of GFP, membranes were blocked overnight at RT in TBSTween20 and 3% nonfat dry milk, followed by probing with a rabbit polyclonal anti-GFP antibody (cat. no. 132002; SySy GmbH, Göttingen, Germany) at RT for 2 h. After three washes with TBSTween20, membranes were incubated at RT for 1 h with a HRP-conjugated donkey anti-rabbit antibody (cat. no. 111-035-003; Dianova) and again washed three times with TBS. ECL detection was conducted as described above.

Immunodetection of PsbO was conducted as for GFP with two exceptions: membranes were blocked in TBSTween20 and 5% nonfat dry milk and incubated with a rabbit polyclonal anti-PsbO primary antibody (E.K. Pistorius University of Bielefeld, Germany).

Analysis of the glycosylation pattern of recombinant proteins was conducted by a ConA assay. Membranes were blocked for 2 min at RT with PBS (140 mM NaCl, 10 mM KCl, 6.4 mM Na_2HPO_4, and 2 mM KH_2PO_4 (pH 7.2)), containing 2% Tween20. After three washes with PBS, membranes were incubated with HRP-conjugated Concanavalin A from *Canavalia ensiformis* (cat. no. L6397; Sigma-Aldrich Chemie GmbH, Munich, Germany) overnight at RT, diluted to a final concentration of 1 μg/ml in PBS, containing 1 mM $CaCl_2$, 1 mM $MnCl_2$, 1 mM $MgCl_2$, and 0.05% Tween20. After three washes with PBS, signals were detected using the ECL system as described above.

RNA analysis

Total RNA was isolated from 100 mg tobacco leaf tissue using Trizol reagent according to the manufacturer's instructions (Thermo Fisher Scientific). RNA integrity was assessed by visualizing the 28S and 18S rRNA bands under UV light in a denaturing 0.8% MOPS-agarose gel containing ethidium bromide. For reverse transcription into complementary DNA (cDNA), total RNA samples were digested with DNase I at 37 °C for 1 h, followed by cDNA synthesis using a commercial kit (RevertAid™ H Minus First Strand cDNA Synthesis Kit (Thermo Fisher Scientific). Two hundred units of reverse transcriptase were added to 5 μg of DNase-treated RNA, 10 mM dNTP mix, 5 μM random hexamer-primer, and

incubated at 42 °C for 1 h. The reaction was stopped by heating to 70 °C for 10 min. PCR was conducted with the DreamTaq DNA polymerase (Thermo Fisher Scientific). Undiluted cDNA (2 μl) were amplified in a 50-μl PCR reaction with the following parameters: after an initial denaturation step (95 °C for 3 min), 35 amplification cycles (95 °C for 30 s, 58 °C for 30 s, and 72 °C for 1.5 min) were carried out and completed by a final elongation step (72 °C for 10 min). The PCR was performed as multiplex assay with construct- and actin-specific primers. Actin, as a housekeeping gene, served as control both for comparison of the quantity of target messenger RNA (mRNA)/cDNA between samples and as control for contamination of samples with genomic DNA. Since the endogenous gene contains an intron, different PCR products were generated from genomic and cDNA templates, with ~1200 and ~850 bp, respectively (Liu et al. 2005). The primer pairs are listed in Table 1.

Ni-NTA purification of cyanophycinases

Purification of the His-tagged recombinant $CphB_{Te}$ and CphE were conducted by immobilized metal affinity chromatography (IMAC) using the ProBond™ Purification System (Thermo Fisher Scientific) and a Ni-chelating resin. Crude *E. coli* or leaf extracts were centrifuged at 16,260×*g* and 4 °C for 1.5 h. A Glass Econo-Column® (1.4 mm diameter; BioRad, Hercules, USA) was packed with 15 ml of the nickel resin. Buffers and samples were loaded onto the column at 2.5 ml/min, employing a peristaltic pump. After an initial equilibration with 150 ml NPI-lysis buffer, containing 10 mM imidazol as described above, variable volumes of extracts were applied, followed by two washing steps with 100 ml NPI buffer, containing 20 and 40 mM imidiazol, respectively. The His-tagged target protein was eluted in five steps each with 5 ml NPI buffer and 300 mM imidazol. Purity of the fractions was checked by applying 20 μl to an SDS-PAGE and subsequent Coomassie staining. Before storing the fractions at −30 °C, fractions were desalted with the help of Sephadex G25M Desalting Columns (Column PD-10; GE Healthcare Europe GmbH; Freiburg, Germany), a desalting buffer (20 mM Tris (pH 8.0) and 1 mM DTT) and a flow rate of 1 ml/min.

Proteolysis assay

In order to investigate the stability of purified CphE, the recombinant protein was incubated in crude *N. benthamiana* leaf extracts. TSP samples were freshly isolated with PBS following the same protocol as for TSP extraction for Western blot analysis. Five nanograms of purified CphE was added to 100 μg TSP of the crude extract, and PBS buffer was added to a final volume of 500 μl. As control CphE was diluted solely in extraction buffer. After incubation for 0, 0.5, 1, 3, or 24 h at RT, samples were precipitated by the addition of 55 μl of a 72% trichloracetic acid solution (TCA) and subsequent incubation for 2 h at 4 °C. Precipitated proteins were pelleted by centrifugation (16,100×*g*; 4 °C; 15 min) and resuspended in 25 μl loading buffer. The pH was adjusted by the addition of 1 μl of saturated Tris solution. Samples were separated in a 12% SDS-PAGE under denaturing conditions, followed by Coomassie staining.

In vitro and semi-in vivo enzyme activity assay

The in vitro enzyme activity assay was carried out according to previously described methods and conditions (Law et al. 2009; Sallam and Steinbüchel 2009a). One micrograms of purified, recombinant protein was added to 20 μg of purified CGP (10 mg/ml in 100 mM HCl), filled with activity buffer (20 mM Tris (pH 7.0) and 1 mM NaOH) to a final volume of 500 μl and incubated for 24 h at RT. After TCA precipitation, samples were loaded onto a 12% SDS-PAGE and Coomassie stained.

For the semi-in vivo assay, leaf tissue from *N. benthamiana* plants was harvested 9 or 11 days post-infiltration (dpi) after transfection with the corresponding vectors and stored on ice. Immediately, crude extracts were prepared with PBS as for the proteolysis assay. Subsequently, 200 μg CGP were added from the stock solution to 1000 μg of TSP samples, PBS was added to a final volume of 500 μl and incubated for 24 h at RT. After TCA precipitation, protein pellets were resuspendend in 250 μl SDS-PAGE loading buffer. Thereof 25 μl, corresponding to 100 μg TSP and 20 μg CGP, were separated in a 12% SDS-PAGE and either Coomassie stained or Western blotted, using GFP and His-Tag-specific antibodies. As control, TSP samples from transgenic plants were incubated without CGP addition under the same conditions. Accordingly, 25 μl of samples were applied to the Western blot for the detection of GFP and CphE, using GFP- and His-Tag-specific antibodies.

In order to determine the enzyme kinetics, 200 μg CGP were diluted either in PBS or 1000 μg of crude TSP extracts of *N. benthamiana*, and 1, 5, and 10 μg of purified CphEal variants or 10, 50, and 100 μg of purified $CphB_{Te}$, respectively, were added. PBS was added to a final volume of 500 μl and incubated at 22–24 °C. At 15 min intervals, one tenth of the original reactions was collected and the reaction stopped by TCA precipitation. Pellets were resuspended in 25 μl SDS-PAGE loading buffer, separated in a 12% SDS-PAGE and subsequently Coomassie stained.

GenBank/EMBL accession no.

The nucleotide sequences of *cphE241bac*, *cphE241syn*, and *cphEalsyn* were deposited in the GenBank nucleotide

database under the accession no. KY131983, KY131981, and KY131982.

Results

Expression and targeting of CphE241 to different cell compartments led to varying accumulation patterns and phenotypic disorders

The expression of CphE in different plant compartments was investigated by transient expression in *N. benthamiana*, using a CphE homolog from *P. alcaligenes* (accession no. JN620418; CphEal). In contrast to the published sequence (Sallam et al. 2011), the *cphE* sequence used in this study, contained an amino acid substitution in the mature protein at position 241 from glycine to aspartic acid (CphE241). The nucleotide sequence was submitted to GenBank under the accession no. KY131983. In silico analysis of the protein stability (MUpro server: http://mupro.proteomics.ics.uci.edu/), tertiary structure (RaptorX server: http://raptorx.uchicago.edu/), and protease target sites (Prosper server: https://prosper.erc.monash.edu.au/home.html) predicted no impact on protein stability, the structure of the catalytic domain, or susceptibility to known proteases.

In order to express the mature CphE241 protein without Sec-leader peptide and with the C-terminal His-Tag in *E. coli* BL21, the vector pET28a-*Cph*Ebac was constructed. The purified enzyme was enzymatically active and served as positive control in Western blots and enzyme activity assays.

After vacuum infiltration of *N. benthaminia* plants with pCphE241bac (cytosol), psR-CphE241bac (plastids), pPec-/pCal-CphE241bac-SEKDEL (ER), and pPec-/pCal-CphE241bac (apoplasm) as well as the empty control vector pICH29912, and pICH18711, encoding cytosolic GFP, plants were harvested from 3 to 13 dpi.

All infiltrated plants displayed phenotypic disorders starting at 5 dpi (Fig. 2a). Plants transfected with the empty vector wilted, leading to complete withering by 9 dpi. In contrast to that, the GFP-expressing replicon did not cause any abnormalities apart from premature yellowing (Fig. 2a). Plants expressing CphE241 with cytosolic, apoplastic, or plastid targeting developed only loosely scattered necrosis. In the case of cytosolic and plastid-targeted CphE241, the number of necroses tended to increase over time. In the case of apoplasm-directed expression, once developed, the number and size of necrosis remained unchanged. Pronounced necrosis and even necrotic sectors occurred on plants infiltrated with the two vectors encoding ER-targeted CphE241 (Fig. 2a). There were no substantial differences between CphE241-SEKDEL fused to the ER-targeting peptides of the apple pectinase and calreticulin (Table 2). For all constructs, symptoms as well as their severity occurred in parallel.

Western blot analysis of crude leaf extracts revealed a differential accumulation pattern depending both on the compartment and the ER-targeting peptide. Cytosolic CphE241 yielded reproducibly the highest accumulation level (Fig. 2b). Recombinant protein could be detected starting at 5 dpi and remained at a constant level up to 13 dpi. In contrast to that, the yield of ER-retained CphE241 was significantly lower for both ER-targeting peptides used. The first faint signals of ER-targeted CGPases could be detected at 5 dpi. Unlike cytosolic CphE241, there was a gradual increase in CphE241 amount up to 11 dpi, declining reproducibly at 13 dpi (Fig. 2b). However, comparing CphE241 translationally fused to the ER-sorting signal of the apple pectinase (pPec-CphE241bac-SEKDEL) and calreticulin (pCal-CphE241bac-SEKDEL), the yield was substantially higher for the Pec-CphE241-SEKDEL. Pec-CphE241 targeted to the apoplasm was found in low amounts between 9 and 13 dpi, paralleling the accumulation pattern of the ER-retrieved counterpart. Apoplasm-targeted Cal-CphE241 could not be detected at all.

In general, yields of apoplasm-targeted proteins were lower compared with the ER-retained counterpart. The accumulation pattern and yield of plastid-targeted CphE241 was comparable with that of cytosolic CphE241. However, the fragments observed in Western blots of crude leaf extracts did not appear reproducibly as distinct bands in contrast to the other CphE241 variants. Moreover, plastid-targeted CphE241 displayed a slightly higher molecular weight compared with the CphE241 protein from *E. coli*, corresponding to the calculated size of unprocessed sR-CphE241 (Fig. 2b; Table 3).

The expression of GFP was approximately 100-fold higher compared with that of cytosolic CphE241 (Fig. 2b). Recombinant protein could already be detected in Western blots at 3 dpi (Fig. 2a).

CphE241 was successfully targeted to the secretory pathway but not to plastids

In order to investigate the correct targeting and processing of CphE241, purified, recombinant proteins were compared in Coomassie-stained SDS-PAGEs. Both ER-retained Pec-CphE241-SEKDEL and Cal-CphE241-SEKDEL displayed a higher molecular weight (Fig. 3a). The difference in size might result either from glycosylation in the ER or from improper processing/translation of the nascent proteins into the ER (Table 3). Sugar residues were specifically detected using a ConA-Western blot (Fig. 3a). In addition, in case of the apple pectinase-sorting determinant, no differences in the fragment size were observed between the ER- and apoplasm-targeted variants (Fig. 3b).

Purified plastid-targeted CphE241 (sR-CphE241) displayed a higher molecular weight as well (Fig. 3a), which correspond to the size of unprocessed protein (Table 3). Similar to the Western blot analysis (Fig. 2b), the bands did

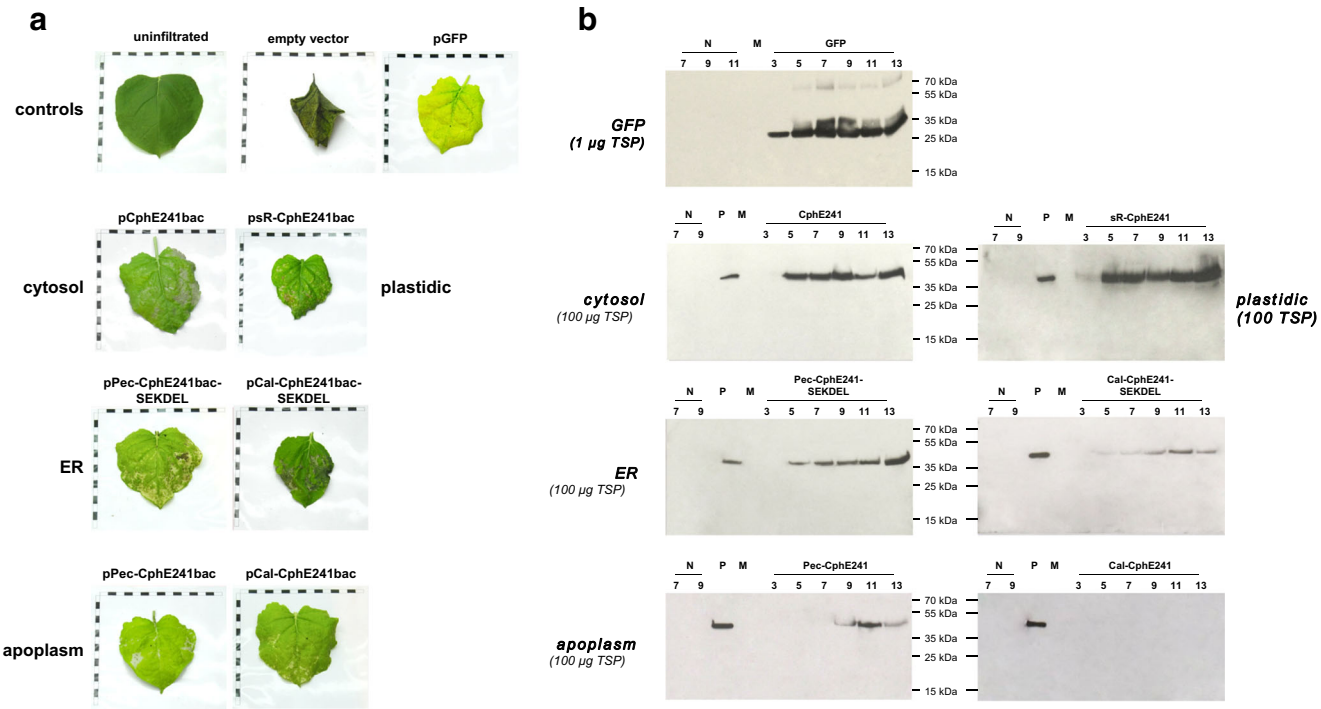

Fig. 2 Characterization of *N. benthamiana* plants, expressing and targeting CphE to different cell compartments. **a** Representative stress symptoms of transfected leaves at 13 dpi; *bar*, 1 cm; **b** Western blots of crude leaf extracts, probed with anti-His antibody for the detection of CphE241 and anti-GFP antibody for detection of GFP. *Numbers* harvest dates post-infiltration; *N* TSP samples from plants, transfected with control vector, *P* 5 ng of purified, recombinant CphE241, produced in *E. coli* BL21, *M* PageRulerPlus Prestained Protein Ladder Mix (Thermo Fisher Scientific)

not appear as distinct, sharp bands. In addition, no signal could be detected for sR-CphE241 in the ConA Western. In order to determine whether sR-CphE241 is retained in the cytosol or translocated to plastids but not processed, plastids were isolated and analyzed by Western blot (Fig. 3c). CphE241 could only be detected in the cytosolic but not in the plastidic fraction. Isolation of plastid proteins was confirmed by immunodetection of PsbO as an endogenous component of photosystem II (Fig. 3c).

Putative reasons for the differential accumulation of cytosolic, ER-targeted, and apoplasm-targeted CphE241

cDNAs were prepared in order to determine the steady-stated level of the viral RNAs, encoding the *cphE241bac* sequences, and amplified by semi-quantitative multiplex-PCR with construct-specific primers and actin primers as a housekeeping gene (Fig. 4a). Since fusion to the RuBisCO small subunit

Table 2 Relative severity of phenotypic abnormalities of plants infiltrated with vectors encoding different variants of *cphe241bac* and the corresponding control vectors

Vector	Localization	3 dpi	5 dpi	7 dpi	9 dpi	11 dpi	13 dpi
Empty vector (pICH29912)	–	–	+	+++	+++++	+++++	+++++
pGFP (pICH18711)	Cytosol	–	+	+	++	++	++
pCphE241bac	Cytosol	–			+	+	++
pPec-CphE241bac-SEKDEL	ER	–	+	++	++	+++	+++
pPec-CphE241bac	Apoplasm	–	+	+	+	+	+
pCal-CphE241bac-SEKDEL	ER	–	+	++	++	+++	+++
pCal-CphE241bac	Apoplasm	–	+	+	+	+	+
psR-CphE241bac	Plastids	–			+	+	++
pCphE241syn	Cytosol	–	+	++	++++	+++++	+++++
pCphEalsyn	Cytosol	–	+	++	++++	+++++	+++++

"+" few scattered necrosis, "++" numerous, scattered necrosis, "+++" extensive necrosis of whole leaf parts and starting symptoms of wilting, "++++" necrosis covering more than 50% of the leaf area and severe wilting, "++++" complete necrosis of all leaves

Table 3 Expected molecular weight of CphE241 fused to different sorting determinants

Localiztation	CphE241 Cytosol	Pec-CphE241-SEKDEL ER	Pec-CphE241 Apoplasm	Cal-CphE241-SEKDEL ER	Cal-CphE241 Apoplasm	sR-CphE241 Plastids
Unprocessed	–	48.2 kDa	47.5 kDa	48.3 kDa	47.6 kDa	51.2 kDa
Processed	44.7 kDa	46.3 kDa + *N*-glycans	44.7 kDa + *N*-glycans	46.3 kDa + *N*-glycans	44.7 kDa + *N*-glycans	44.7 kDa

transit peptide failed to target CphE241 to the plastids, this construct was not analyzed further. There were no significant differences in the amount of RNA encoding cytosolic CphE241 and pPec-CphE241bac-SEKDEL. The trend of the RNA of pCal-CphE241bac-SEKDEL seems to be reduced in comparison with the other transgene-encoding RNAs, which is particularly true for later harvest dates (9–13 dpi).

Differences in the accumulation pattern might also result from differing stability of the recombinant protein and/or their susceptibility to endogenous plant proteases. In order to determine whether this is due to the C-terminal SEKDEL-retrieval signal or the glycosylation pattern, purified CphE241 variants were incubated in crude leaf extracts from uninfiltrated *N. benthamiana* plants for up to 24 h (Fig. 4b). CphE241 (Fig. 4b) and $CphB_{Te}$ (Fig. S3) isolated from *E. coli* BL21 served as controls. Unglycosylated CphE241, produced in the cytosol of *E. coli* and *N. benthamiania*, was not degraded in the time investigated, whereas $CphB_{Te}$ could not be detected after 3 h (Fig. S3). Glycosylated CphE241 variants with and without SEKDEL-retrieval signal were stable for up to 3 h, but undetectable after 24 h. Fusion to the signal peptide of small subunit of RuBisCO and improper processing did not affect the protein stability. sR-CphE241 demonstrated resistance to endogenous proteases similar to the cytosol-targeted version (Fig. S4).

CphE241 variants are enzymatically active under in vitro and semi in vivo conditions

Apart from effects on the protein stability, differences in the sequence and the glycosylation pattern might have an impact on the enzymatic activity of the CphE241 variants targeted to the cytosol, ER, apoplasm, and plastids. Thus, purified CphE241s were incubated with isolated CGP, which was completely degraded after 24 h in all cases (Fig. 5a; Fig. S5).

In parallel, purified CGP was added to crude extracts from *N. benthamiana* plants transfected with the different constructs and incubated for 24 h at RT. In all CphE241-containing extracts, including unprocessed sR-CphE241, CGP was degraded after 24 h (Fig. 5b; Fig. S5). Presence of recombinant GFP and CphE241 proteins were confirmed by GFP- and His-Western blot, respectively (Fig. 5c).

Amino acid substitution did not affect CphE expression and yield

In order to determine the putative effect of the point mutation, which led to an amino acid substitution from G to D at position 241, two synthetic coding regions were designed, which differ only in the corresponding codon, named *cphE241syn* and *cphEalsyn*, respectively. In addition, the synthetic

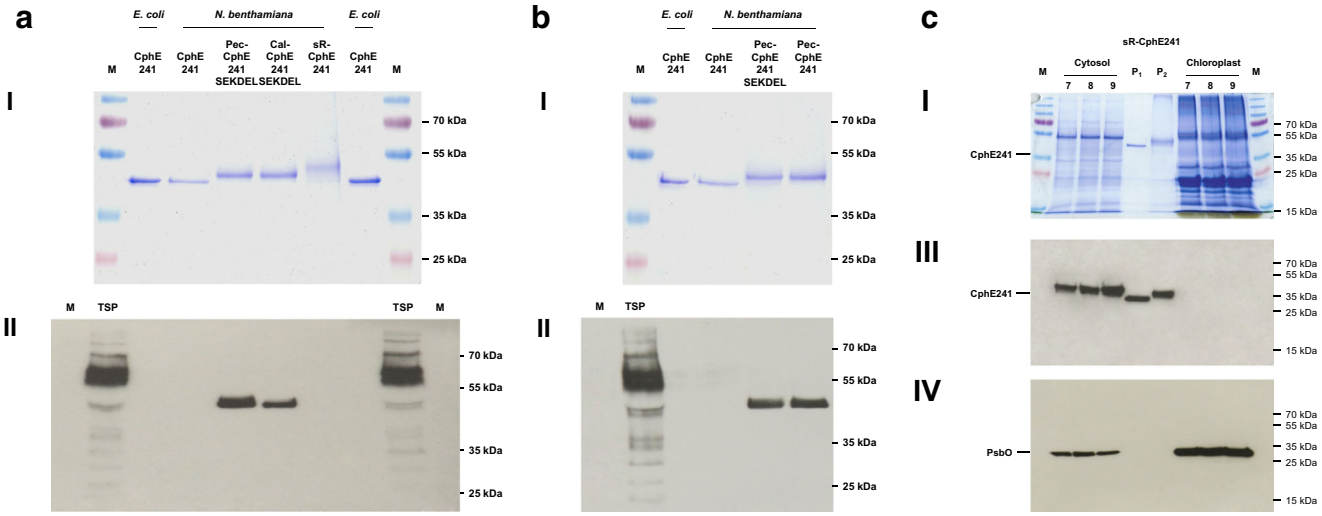

Fig. 3 Characterization of CphE241 targeted to different cell compartments. *I* Coomassie-stained SDS-PAGE; *II* ConA-, *III* His-, and *IV* PsbO-Western blot of **a** purified CphE241 variants, **b** ER- and apoplasm-targeted Pec-CphE241, and **c** cytosolic and plastidic fraction of sR-CphE241. *P1* purified cytosolic CphE241, *P2* purified plastid-targeted sR-CphE241, *M* PageRuler Plus Prestained Protein Ladder Mix (Thermo Fisher Scientific), *TSP* total soluble protein; *Numbers* days post-infiltration

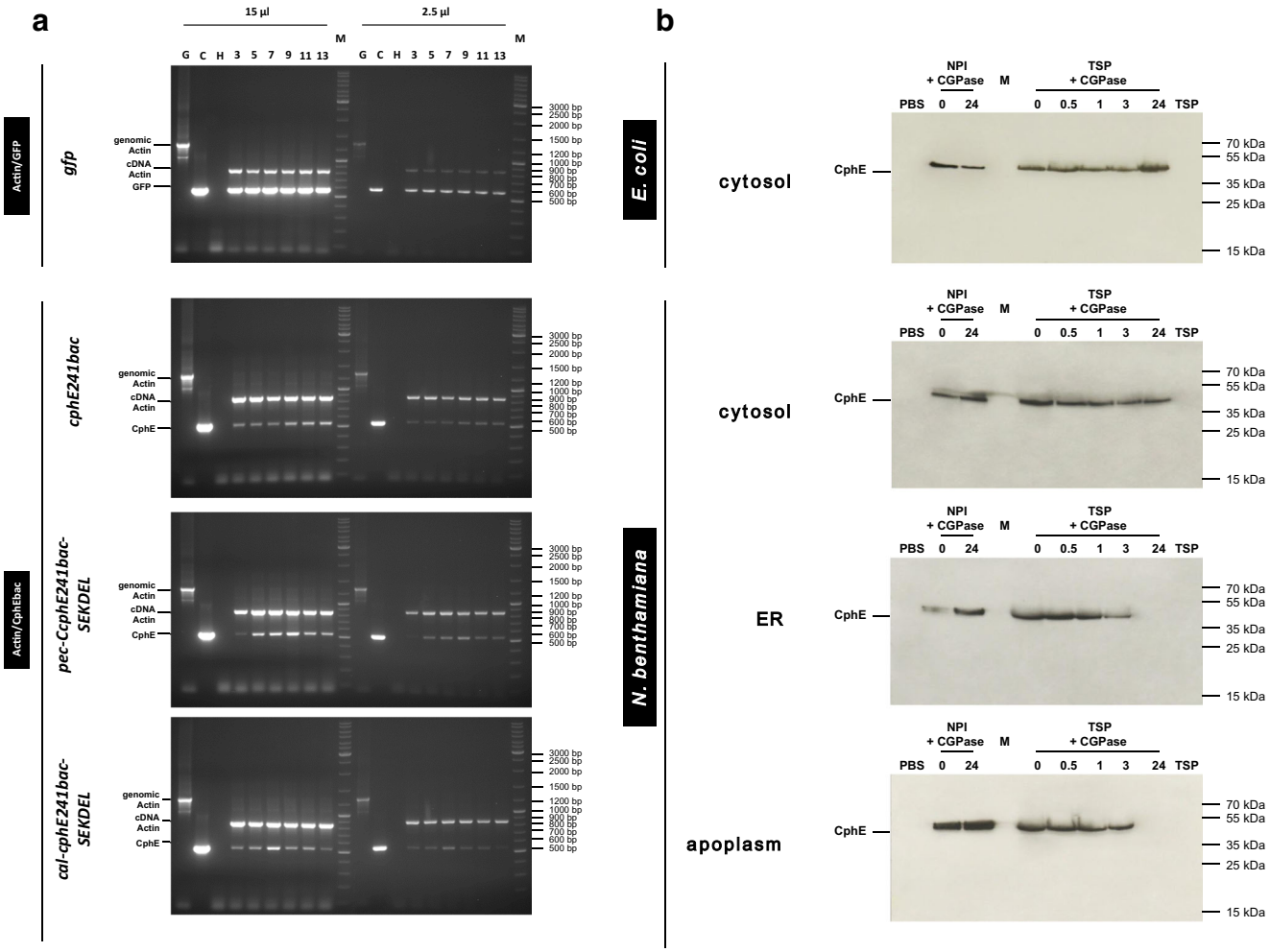

Fig. 4 Analysis of the transcript levels and the proteolytic susceptibility of CphE241 RNA and protein. **a** Semi-quantitative multiplex-PCR (15 and 2.5 µl of each reaction). Primer and samples are specified at the left site; *G* samples of genomic DNA from uninfiltrated *N. benthamiana* plants, *C* plasmid DNA used for the transient expression, *H A. dest* control; *Numbers* harvest dates post-infiltration. **b** Proteolysis assay with purified CphE241 variants CGPase/purified CphE241; *TSP* total soluble protein, *NPI* extraction buffer used for the isolation of TSP samples; *Numbers* incubation times (h)

sequence was adapted to the codon usage of *Nicotiana*. The nucleotide sequences were submitted to GenBank under the accession no. KY131981 and KY131982. Both coding regions were introduced into the MagnICON vector, leading to cytosolic expression.

N. benthamiana plants infiltrated with p*cphE241syn* and p*cphEalsyn* displayed equally severe phenotypic stress symptoms (Fig. 6a; Table 2). First, necrosis appeared at 5 dpi, rapidly increasing in severity, leading to complete wilting of the entire plant after 9 dpi. Plants transfected with GFP-expressing control vector again displayed only mild symptoms as described above.

Differences in the expression pattern were determined both in terms of protein accumulation (Fig. 6b, c) and at the steady-state level of the corresponding viral RNAs (Fig. 6d). Western blots of dilution series of the crude TSP extracts, ranging from 100 to 1 µg TSP per sample/lane, showed no difference in the accumulation of the "synthetic" variants and showed yields which were similar to that of GFP. CphE241 and CphEal could be detected even when applying only 1 µg of TSP to Western blots (Fig. 6b). In comparison with the vector encoding the bacterial sequence *cphE241bac*, protein yields of "synthetic" CphE variants were approximately 100-fold higher. In contrast to those, CphE241, encoded by the bacterial sequence, could only be detected when applying 100 µg of TSP to Western blot analysis. Differences in the yield became more evident when applying the same amounts of TSP (Fig. 6c). Using 10 µg of TSP, signals of the "bacterial" CphE241 were only barely visible, whereas lanes were overloaded by the synthetic CphE variants. Furthermore, the first signals of the synthetic CphEs were already detectable at 3 dpi, whereas the bacterial CphE241 could not be detected before 5 dpi (Figs. 2b and 6b).

The steady-state level of the RNAs of *cphE241syn* and *cphEalsyn* paralleled that of the protein, and no differences between the two RNAs were observed. Transcript

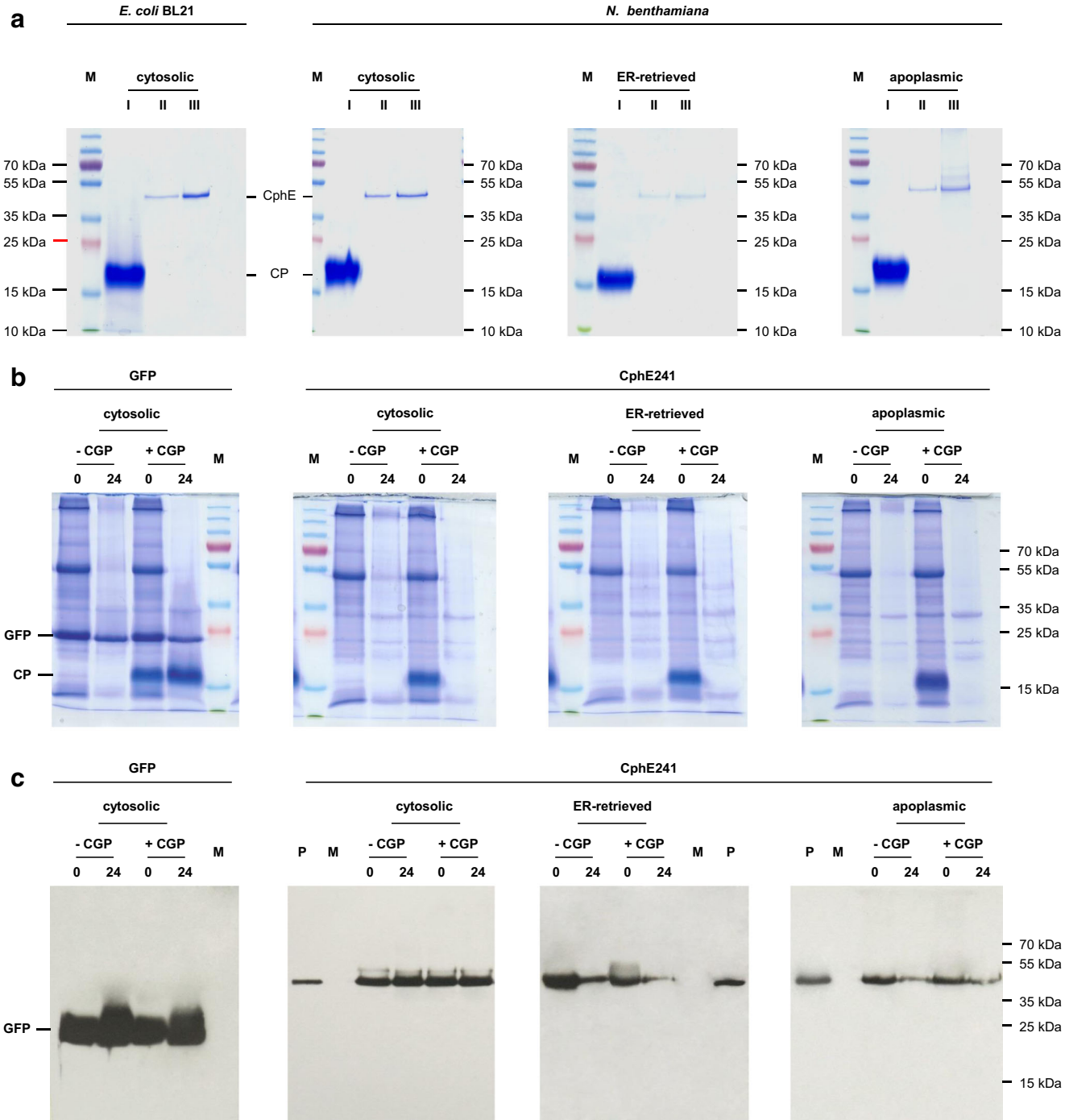

Fig. 5 CphE241 enzyme activity assay under in vitro and *semi*-in vivo conditions. *M* PageRuler Plus Prestained Protein Ladder. **a** In vitro assay, 20 μg of CGP incubated with 1 μg purified CphE241 for 24 h at RT: *I* 20 μg CGP; *II* 20 μg CGP + 1 μg CphE241; *III*, 1 μg CphE241. **b** Semi-in vitro assay—20 μg CGP incubated in 100 μg crude TSP extracts of *N. benthamiana*, transfected with vectors, encoding either GFP or the different CphE241 variants. *Numbers* incubation time (h). **c** Western blot of samples of the semi-in vivo activity assay using GFP- and His-tag-specific antibodies. *P* 5 ng of CphE241-purified *E. coli* BL21; *Numbers* incubation time (h).

accumulation nearly reached that of GFP. Hence, RNA levels were higher by several orders of magnitude, compared with the viral RNA encoding the bacterial *cphE241bac* sequence, as demonstrated by the relative ratio to the actin mRNA as housekeeping gene (Fig. 6d), indicating that codon-optimization significantly boosted reverse transcription.

Amino acid substitution affected the enzyme activity neither in vitro nor in crude leaf extracts of *N. benthamiana*

In order to compare CphE with and without amino acid substitution in terms of their enzyme activities and

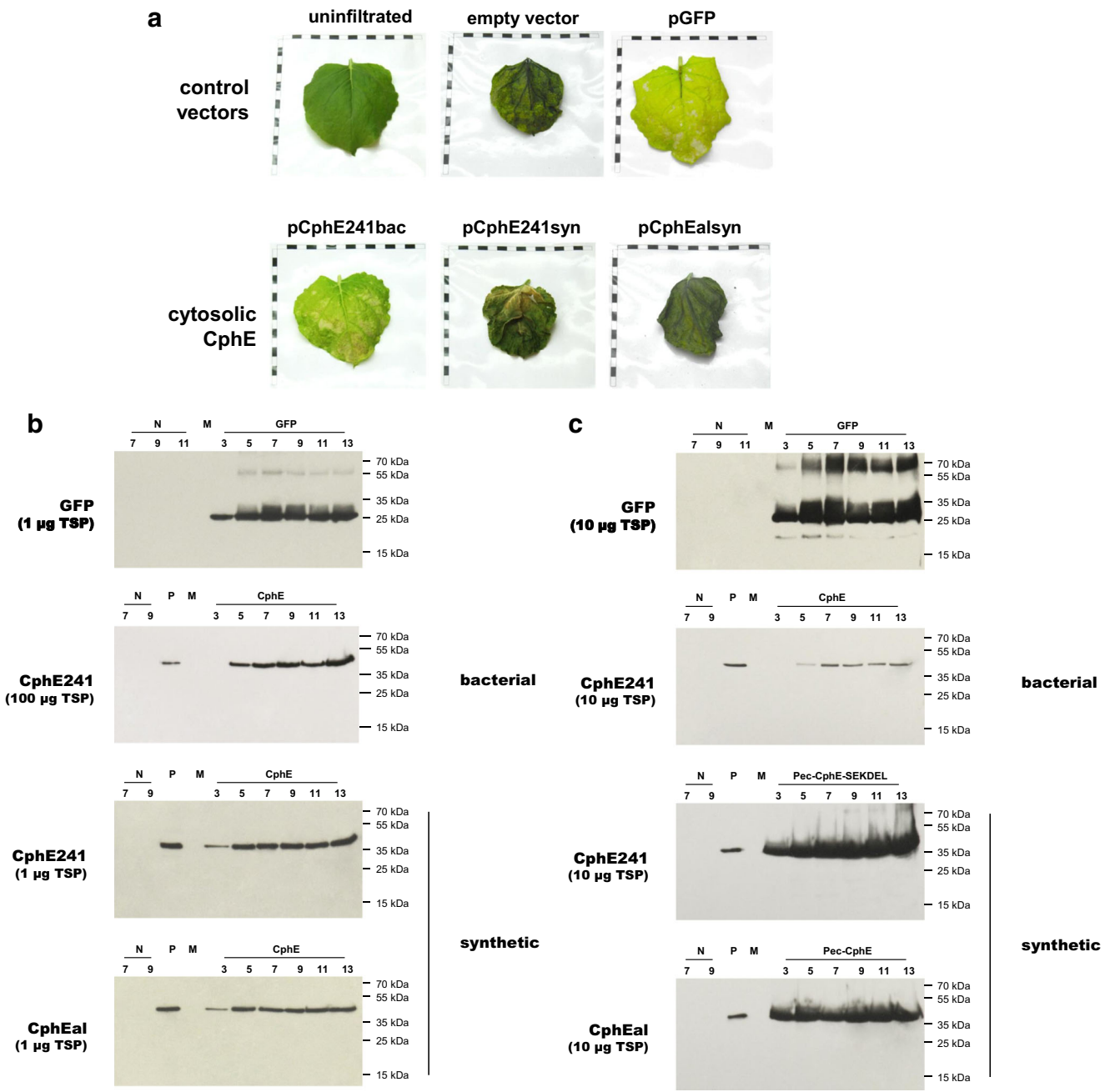

Fig. 6 Comparison of cytosolic CphE with and without amino acid substitution. **a** Representative stress symptoms of transfected leaves at 13 dpi; **b**, **c** Western blots with different amounts of crude leaf extracts, probed with anti-His and anti-GFP antibody for the detection of CphE and GFP, respectively. *Numbers* harvest dates post-infiltration; *N* TSP samples from plants, transfected with the control vector; *P* 5 ng of purified, recombinant CphE241, produced in *E. coli* BL21, *M* PageRuler Plus Prestained Protein Ladder Mix (Thermo Fisher Scientific). **d** Semi-quantitative multiplex-PCR (15 and 2.5 µl of each reaction). Primer and samples are specified at the left site; *G* samples of genomic DNA from uninfiltrated *N. benthamiana* plants, *C* plasmid DNA used for the transient expression, *H A. dest* control reaction, numbers harvest dates post-infiltration

kinetics, the proteins were purified by IMAC from leaf tissue and subjected to an in vitro activity assay. Two hundred micrograms of CGP were incubated with different amounts of recombinant CphE variants (1, 5, and 10 µg), and a tenth of the reaction mixture was collected at intervals of 15 min. There were no significant differences between both enzyme variants under in vitro conditions (Fig. 7a–c). Degradation of CGP was still detectable within 120 min when the ratio of of CphE to CGP was reduced to 1/200 (20 µg CGP/100 ng CphE). Interestingly, recombinant $CphB_{Te}$, purified from *E. coli* BL21, proved to be less active. Twenty micrograms CGP

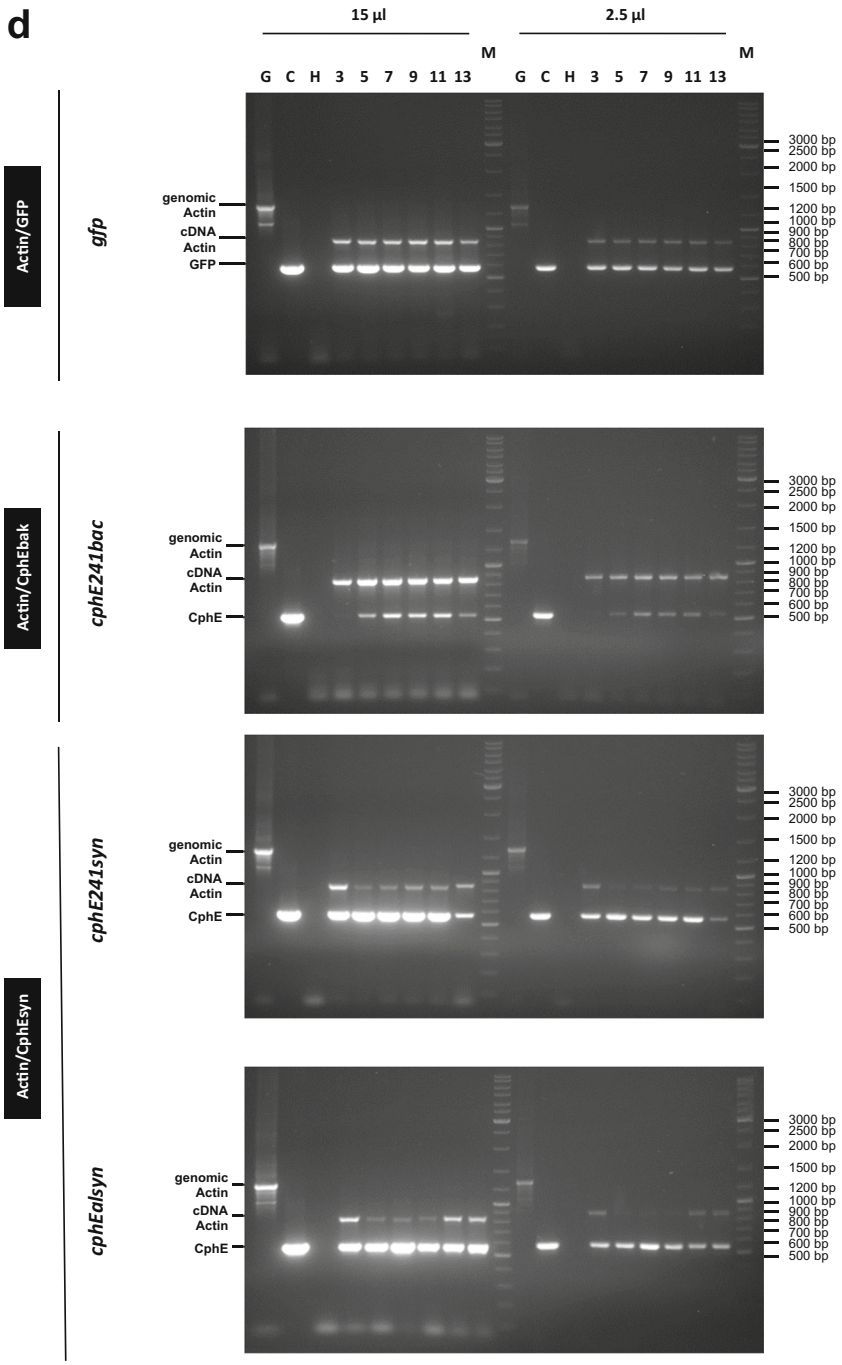

Fig. 6 (continued)

was degraded by 5 µg $CphB_{Te}$ within 75 min (Fig. S6), whereas the same amount of CGP was degraded by 500 ng of both CphE variants within 30 min. Two hundred fifty nanograms of CphE demonstrated an enzyme activity comparable with that of 5 µg $CphB_{Te}$ (data not shown).

Since there was no difference in the enzyme activity of CphE241 and CphEal under in vitro conditions, further analyses were only done with CphE241. In order to determine the enzyme kinetics of the mutated CphE241 in crude leaf extracts of *N. benthamiana*, 200 µg of CGP were added to 1 mg of crude TSP extracts and incubated again with 1, 5, or 10 µg of cyanophycinase (Fig. 7d, e). For each sample, a tenth of the reaction mixture was collected every 15 min. CGP degradation pattern was comparable with that of the in vitro assay (Fig. 7c, e).

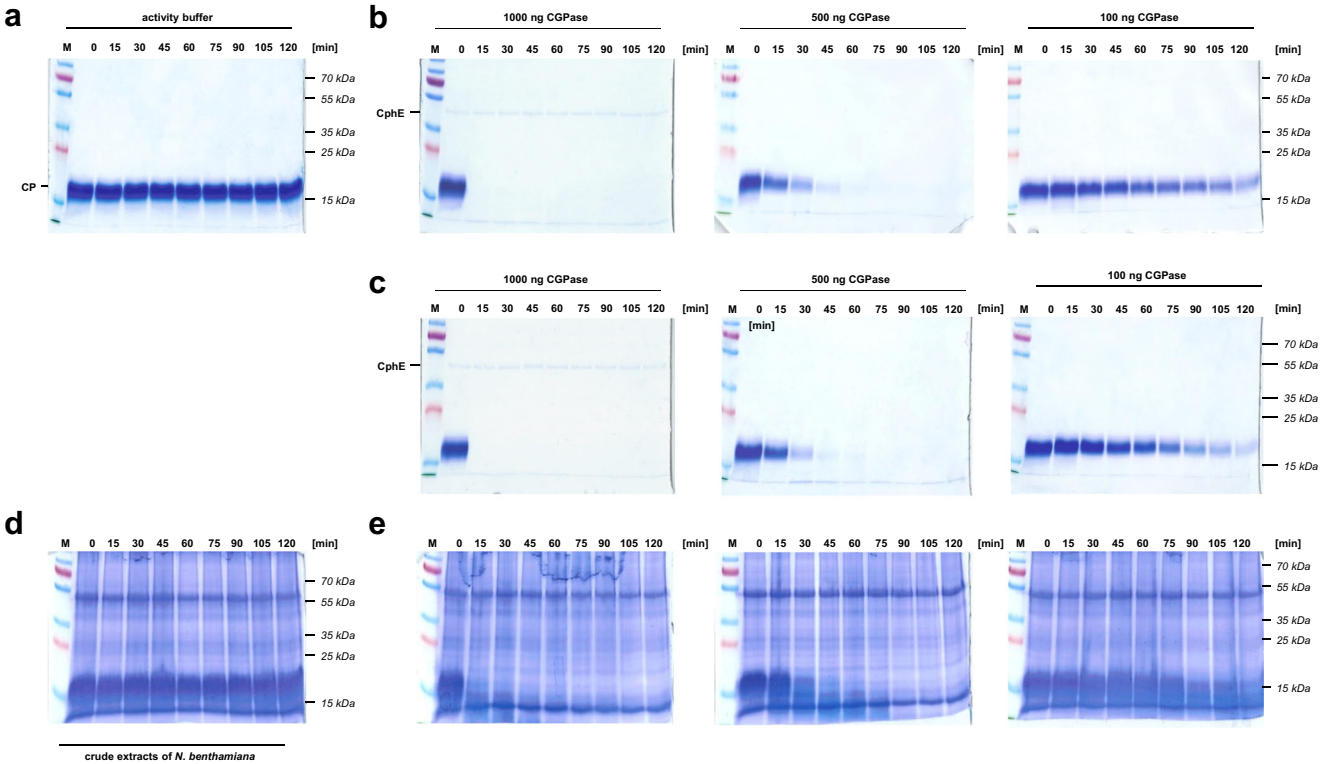

Fig. 7 Comparison of the enzyme kinetic of mutated and native CphEal under in vitro conditions and in crude leaf extracts from *N. benthamiana*. Twenty micrograms of isolated CGP per lane, incubated either in enzyme activity buffer or 100 μg of crude TSP extracts from *N. benthamiana*, without any cyanophycinase (**a**, **d**) or with 100, 500, and 1000 ng of recombinant-purified CphEal (**b**) or CphE241 (**c**, **e**). *Numbers*, minutes at which the reaction was stopped. *Marker* PageRuler Plus Prestained Protein Ladder Mix (Thermo Fisher Scientific)

Discussion

CphEal from *P. alcaligenes* DIP-1 (Sallam et al. 2011) and its mutated variant CphE241 were similar in yield (Fig. 6b, c) and enzyme activity (Fig. 7b, c) when expressed in *N. bentamiana*. Thus, the amino acid substitution had no detectable effect and the two proteins were assumed to be equal in the study.

When targeted to the plant cytosol, CphE241 accumulated at moderate levels. Codon optimization of the coding region boosted the yield substantially (Fig. 6b, c) and levels were obtained that were comparable with that of cytosolic GFP. The increase seemed to result from a higher transcript level (Fig. 6d). This would be in line with Barahimipour et al. (2015) who demonstrated that the adaptation of codons and GC content prevented a heterochromatinization of the transgene locus and improved mRNA stability as well as translatability (Barahimipour et al. 2015).

The CphE yield was significantly higher compared with the CGPase $CphB_{Te}$, which was also expressed in the cytosol of *N. benthamiana* (Ponndorf et al. 2016). Even though the same MagnICON vector was used to express a codon-optimized *cph*B_{Te} sequence, the recombinant $CphB_{Te}$ could only be detected in Western blots when using 50 μg of TSP, whereas in case of CphE 1 μg of TSP was sufficient. This might be caused by the resistance of cytosolic CphE to proteolytic degradation in crude plant extracts (Fig. 4b) whereas $CphB_{Te}$ was rapidly degraded (Fig. S3). Ponndorf et al. (2016) had to fuse $CphB_{Te}$ to stabilizing partners such as GFP in order to increase yields. Since both types of CGPases, even though catalyzing the same reaction, are unrelated (Sallam et al. 2011), the differing susceptibility to plant proteases might be an attribute of the evolutionary adaptation of the amino acid sequences to the milieus in which they naturally occur. CphB-type CGPases are intracellular enzymes, whereas CphEs are secreted. Due to the substantially higher proteolytic activity in the extracellular space compared with the cytosol (Benchabane et al. 2008; Gómez and Pallás 2010; Goulet et al. 2012; Pillay et al. 2014; Robert et al. 2013), secretory proteins require a higher resistance.

However, when targeted to the apoplasm, CphE accumulated only in low amounts (Fig. 2b) and apoplasmic — in contrast to cytosolic — CphE was degraded in crude plant extracts (Fig. 4b). This could be due to the glycosylation that does not occur in the bacterial protein. The impact of glycosylation on protein stability is well documented by Solá and Griebenow (2009). Moreover, Stevens et al. (2000) and Delannoy et al. (2008) showed that plant-derived proteins degraded more rapidly in tobacco leaf extracts when comparing the stability of identical antibodies, either made by plant or murine cells.

A negative impact of the glycosylation would also explain the sensitivity of ER-targeted CphE (Fig. 4b) to plant proteases and hence the moderate accumulation levels compared with the cytosolic variant (Fig. 2b). In line with this, Duwadi et al. (2015) reported that recombinant proteins were degraded by ER-resident proteases (Duwadi et al. 2015). Nevertheless, this is in contrast to the majority of publications demonstrating that targeting to the ER benefits the yield of recombinant protein, ascribed to the lower amount of proteases and the more abundant molecular chaperones (Benchabane et al. 2008; Goulet et al. 2012; Lallemand et al. 2015; Pillay et al. 2014; Sainsbury et al. 2013).

The fact that the expression of ER-targeted CphE induced severe phenotypical disorders (Fig. 2a) implies that the recombinant protein interfered with the endogenous metabolism that is exclusively present in the ER. Leaf necrosis caused by cytotoxic effects of transiently expressed proteins have already been reported for other recombinant, ER-targeted proteins, such as an unglycosylated cholera toxin B (Hamorsky et al. 2015), the human complement factor C5a (Nausch et al. 2012), LTB-MUC1 (Pinkhasov et al. 2011), and the hepatitis B core antigen (Huang et al. 2006). In all cases, cytotoxic effects led to low amounts of the target proteins, below 0.1% of TSP (Hamorsky et al. 2015; Huang et al. 2006; Nausch et al. 2012; Pinkhasov et al. 2011). Moreover, Badri et al. (2009) related the phenotypic stress symptoms that were induced by an ER-directed recombinant protein, to an inhibition of the overall protein synthesis (Badri et al. 2009). The authors assumed that high amounts of a newly synthesized recombinant protein exceeded the capacity of ER-localized chaperones to fold the proteins, inducing the unfolded protein response (UPR) which reduces the protein synthesis until it is balanced to the capacity of chaperones (Hussain et al. 2014; Thomas and Walmsley 2014). Hence, the lower accumulation level of ER-directed CphE might not only be caused by a higher susceptibility to proteases but also by the induction of the UPR.

Depending on the ER-targeting peptide, significant differences in the accumulation level of secretory CphE were observed. The translational fusion to the signal of the apple pectinase yielded higher amounts compared with the fusion with the calreticulin leader peptide (Fig. 2b). It might be assumed that the calreticulin signal peptide negatively affects the translation, since translocation into the ER is a co-translational process. The transfer efficiencies of the different leader peptides might differ, causing a differential delay in translation and thus varying yields. This hypothesis is supported by the fact that the same ER-sorting determinants led to similar differences in the accumulation level of another recombinant target protein as well as ten other ER-targeting signals (Hamorsky et al. 2013). However, this difference was not observed in other studies, indicating that the combination of transit peptide and target proteins is relevant as well (He et al. 2014; Kalthoff et al. 2010; Marillonnet et al. 2004; Santi et al. 2006, 2008; Teh and Kavanagh 2010; Webster et al. 2009).

Analysis of the molecular size of purified CphE variants suggest that plastid-targeted CphE was not processed (Fig. 3a). Similar effects have already been reported for other proteins fused to the same synthetic RuBisCO transit peptide (Kalthoff et al. 2010; Ponndorf et al. 2016; Webster et al. 2009). Though, in contrast to CphE, processed forms of these proteins were always found as well. However, for CphE, no mature protein could be detected in crude extracts and no recombinant protein at all in isolated plastids (Fig. 3c). Thus, translocation and processing seemed to be completely impaired in this case, demonstrating that the recognition of the sR transit peptide seems to be affected by the target protein fused to it.

The capability of purified CphE to degrade CGP was not affected in crude extracts of *N. benthamiana* compared with the activity under in vitro conditions (Fig. 7c, e). More important is the fact that moderate accumulation levels of CphE in crude plant extracts — achieved by transient expression — were able to degrade substantial amounts of CGP as well (Fig. 5b).

The fact that 20 times more $CphB_{Te}$ was necessary to degrade the same amount of CGP compared with CphE under in vitro conditions (Fig. S6) cannot be due to enzyme stability since both were similarly stable under in vitro conditions, but instead indicates a higher specific activity of CphE.

Therefore, CphE is a suitable candidate for stable expression in CGP-producing plants in order to allow induced CGP degradation *in planta.* Due to this spatial separation, plastidic CGP should be unaffected by the enzymes as long as the cells are intact, but degraded during animal feeding, when chloroplasts are decomposed.

Acknowledgements We thank Prof. Dr. Steinbüchel (Institut für Molekulare Mikrobiologie und Biotechnologie, Westfälische Wilhelms-Universität, Münster, Germany) and Dr. Krehenbrink (Cysal GmbH, Münster, Germany) for providing the CphE encoding plasmid. Likewise, we thank Dr. Gleba and Dr. Giritch (Nomad BioScience; Halle/Saale, Germany) for the MagnICON expression vectors and for their constructive discussions. In addition, we would like to express the warmest of thanks to Alex Rajewski for thoroughly proof-reading the manuscript and the helpful suggestions and comments.

Compliance with ethical standards

Funding The authors did not receive any funding.

Conflict of interest The authors declare that they have no conflict of interest.

Ethical approval This article does not contain any studies with human participants or animals performed by any of the authors.

References

Arai Y, Shikanai T, Doi Y, Yoshida S, Yamaguchi I, Nakashita H (2004) Production of Polyhydroxybutyrate by polycistronic expression of bacterial genes in tobacco plastid. Plant Cell Physiol 45(9):1176–1184. doi:10.1093/pcp/pch139

Badri MA, Rivard D, Coenen K, Michaud D (2009) Unintended molecular interactions in transgenic plants expressing clinically useful proteins: the case of bovine aprotinin traveling the potato leaf cell secretory pathway. Proteomics 9(3):746–756. doi:10.1002/pmic.200700234

Barahimipour R, Strenkert D, Neupert J, Schroda M, Merchant SS, Bock R (2015) Dissecting the contributions of GC content and codon usage to gene expression in the model alga *Chlamydomonas reinhardtii*. Plant J 84(4):704–717. doi:10.1111/tpj.13033

Benchabane M, Goulet C, Rivard D, Faye L, Gomord V, Michaud D (2008) Preventing unintended proteolysis in plant protein biofactories. Plant Biotechnol J 6(7):633–648. doi:10.1111/j.1467-7652.2008.00344.x

Bendandi M, Marillonnet S, Kandzia R, Thieme F, Nickstadt A, Herz S, Fröde R, Inogés S, Lòpez-Dìaz de Cerio A, Soria E, Villanueva H, Vancanneyt G, McCormick A, Tusé D, Lenz J, Butler-Ransohoff J-E, Klimyuk V, Gleba Y (2010) Rapid, high-yield production in plants of individualized idiotype vaccines for non-Hodgkin's lymphoma. Ann Oncol 21(12):2420–2427. doi:10.1093/annonc/mdq256

Broer S (2008) Amino acid transport across mammalian intestinal and renal epithelia. Physiol Rev 88(1):249–286. doi:10.1152/physrev.00018.2006

Chen H, Wong EA, Webb KE (1999) Tissue distribution of a peptide transporter mRNA in sheep, dairy cows, pigs, and chickens. J Anim Sci 77(5):1277–1283

Delannoy M, Alves G, Vertommen D, Ma J, Boutry M, Navarre C (2008) Identification of peptidases in *Nicotiana tabacum* leaf intercellular fluid. Proteomics 8(11):2285–2298. doi:10.1002/pmic.200700507

Duwadi K, Chen L, Menassa R, Dhaubhadel S (2015) Identification, characterization and down-regulation of cysteine protease genes in tobacco for use in recombinant protein production. PLoS One 10(7). doi:10.1371/journal.pone.0130556

Fan P, Wang X, Kuang T, Li Y (2009) An efficient method for the extraction of chloroplast proteins compatible for 2-DE and MS analysis. Electrophoresis 30(17):3024–3033. doi:10.1002/elps.200900172

FAO (2014) pigs and nutrition and feed

Frommeyer M, Wiefel L, Steinbüchel A (2014) Features of the biotechnologically relevant polyamide family "cyanophycins" and their biosynthesis in prokaryotes and eukaryotes. Crit Rev Biotechnol 0(0):1–12. doi:10.3109/07388551.2014.946467

Gómez G, Pallás V (2010) Noncoding RNA mediated traffic of foreign mRNA into chloroplasts reveals a novel signaling mechanism in plants. PLoS One 5(8):e12269. doi:10.1371/journal.pone.0012269

Goulet C, Khalf M, Sainsbury F, D'Aoust M-A, Michaud D (2012) A protease activity-depleted environment for heterologous proteins migrating towards the leaf cell apoplast. Plant Biotechnol J 10(1):83–94. doi:10.1111/j.1467-7652.2011.00643.x

Güttler S (2008) Forschung und Entwicklung in der Aquakultur - Ein Überblick über Arbeitsgebiete und offene Fragen. Innovation & Information Working Paper; Institut für Agrarökonomie; Christian-Albrechts-Universität Kiel doi:http://www.agric-econ.uni-kiel.de/Abteilungen/II/wp.shtml

Hamorsky KT, Kouokam JC, Bennett LJ, Baldauf KJ, Kajiura H, Fujiyama K, Matoba N (2013) Rapid and scalable plant-based production of a cholera toxin B subunit variant to aid in mass vaccination against cholera outbreaks. PLoS Negl Trop Dis 7(3):e2046. doi:10.1371/journal.pntd.0002046

Hamorsky KT, Kouokam JC, Jurkiewicz JM, Nelson B, Moore LJ, Husk AS, Kajiura H, Fujiyama K, Matoba N (2015) N-glycosylation of cholera toxin B subunit in *Nicotiana benthamiana*: impacts on host stress response, production yield and vaccine potential. Scientific Reports 5. doi:10.1038/srep08003

He J, Peng L, Lai H, Hurtado J, Stahnke J (2014) Chen Q (2014) a plant-produced antigen elicits potent immune responses against west nile virus in mice. Biomed Res Int. doi:10.1155/2014/952865

Huang Z, Santi L, LePore K, Kilbourne J, Arntzen CJ, Mason HS (2006) Rapid, high-level production of hepatitis B core antigen in plant leaf and its immunogenicity in mice. Vaccine 24(14):2506–2513. doi:10.1016/j.vaccine.2005.12.024

Huhns M, Neumann K, Hausmann T, Klemke F, Lockau W, Kahmann U, Kopertekh L, Staiger D, Pistorius EK, Reuther J, Waldvogel E, Wohlleben W, Effmert M, Junghans H, Neubauer K, Kragl U, Schmidt K, Schmidtke J, Broer I (2009) Tuber-specific *cph*A expression to enhance cyanophycin production in potatoes. Plant Biotechnol J 7(9):883–898. doi:10.1111/j.1467-7652.2009.00451.x

Huhns M, Neumann K, Hausmann T, Ziegler K, Klemke F, Kahmann U, Staiger D, Lockau W, Pistorius EK, Broer I (2008) Plastid targeting strategies for cyanophycin synthetase to achieve high-level polymer accumulation in *Nicotiana tabacum*. Plant Biotechnol J 6(4):321–336. doi:10.1111/j.1467-7652.2007.00320.x

Huhns M, Neumann K, Lockau W, Ziegler K, Pistorius EK, Broer I (2004) Bioplastic in transgenic plants: cyanophycin as a suitable resource for polyaspartate. Paper presented at the Agricultural Biotechnology International Conference, Cologne, Germany

Hussain H, Maldonado-Agurto R, Dickson AJ (2014) The endoplasmic reticulum and unfolded protein response in the control of mammalian recombinant protein production. Biotechnol Lett 36(8):1581–1593. doi:10.1007/s10529-014-1537-y

Kalthoff D, Giritch A, Geisler K, Bettmann U, Klimyuk V, Hehnen HR, Gleba Y, Beer M (2010) Immunization with plant-expressed hemagglutinin protects chickens from lethal highly pathogenic avian influenza virus H5N1 challenge infection. J Virol 84(22):12002–12010. doi:10.1128/JVI.00940-10

Klang JE, Burnworth LA, Pan YX, Webb KE Jr, Wong EA (2005) Functional characterization of a cloned pig intestinal peptide transporter (pPepT1). J Anim Sci 83(1):172–181

Klemke F, Nürnberg DJ, Ziegler K, Beyer G, Kahmann U, Lockau W, Volkmer T (2016) CphA2 is a novel type of cyanophycin synthetase in N2-fixing cyanobacteria. Microbiology (United Kingdom) 162(3):526–536. doi:10.1099/mic.0.000241

Lallemand J, Bouché F, Desiron C, Stautemas J, de Lemos EF, Périlleux C, Tocquin P (2015) Extracellular peptidase hunting for improvement of protein production in plant cells and roots. Front Plant Sci 6. doi:10.3389/fpls.2015.00037

Law AM, Lai SWS, Tavares J, Kimber MS (2009) The structural basis of β-peptide-specific cleavage by the serine protease cyanophycinase. J Mol Biol 392(2):393–404. doi:10.1016/j.jmb.2009.07.001

Liu J-Z, Blancaflor EB, Nelson RS (2005) The tobacco mosaic virus 126-kilodalton protein, a constituent of the virus replication complex, alone or within the complex aligns with and traffics along microfilaments. Plant Physiol 138(4):1853–1865. doi:10.1104/pp.105.065722

Lu H, Klaassen C (2006) Tissue distribution and thyroid hormone regulation of Pept1 and Pept2 mRNA in rodents. Peptides 27(4):850–857. doi:10.1016/j.peptides.2005.08.012

Marillonnet S, Giritch A, Gils M, Kandzia R, Klimyuk V, Gleba Y (2004) *In planta* engineering of viral RNA replicons: efficient assembly by recombination of DNA modules delivered by *Agrobacterium*. Proc Natl Acad Sci U S A 101(18):6852–6857. doi:10.1073/pnas.0400149101

Nakamura Y, Kaneko T, Sato S, Ikeuchi M, Katoh H, Sasamoto S, Watanabe A, Iriguchi M, Kawashima K, Kimura T, Kishida Y, Kiyokawa C, Kohara M, Matsumoto M, Matsuno A, Nakazaki N, Shimpo S, Sugimoto M, Takeuchi C, Yamada M, Tabata S (2002) Complete genome structure of the thermophilic cyanobacterium *Thermosynechococcus elongatus* BP-1. DNA Res 9(4):123–130. doi:10.1093/dnares/9.4.123

Nausch H, Hausmann T, Ponndorf D, Hühns M, Hoedtke S, Wolf P, Zeyner A, Broer I (2016a) Tobacco as platform for a commercial production of cyanophycin. New Biotechnol 33(6):842–851. doi:10.1016/j.nbt.2016.08.001

Nausch H, Huckauf J, Broer I (2016b) Peculiarities and impacts of expression of bacterial cyanophycin synthetases in plants. Appl Microbiol Biotechnol 100(4):1559–1565. doi:10.1007/s00253-015-7212-y

Nausch H, Mischofsky H, Koslowski R, Meyer U, Broer I, Huckauf J (2012) Expression and subcellular targeting of human complement factor C5a in *Nicotiana* species. PLoS One 7(12). doi:10.1371/journal.pone.0053023

Pillay P, Schlüter U, van Wyk S, Kunert KJ, Vorster BJ (2014) Proteolysis of recombinant proteins in bioengineered plant cells. Bioengineered 5(1):15–20. doi:10.4161/bioe.25158

Pinkhasov J, Alvarez ML, Rigano MM, Piensook K, Larios D, Pabst M, Grass J, Mukherjee P, Gendler SJ, Walmsley AM, Mason HS (2011) Recombinant plant-expressed tumour-associated MUC1 peptide is immunogenic and capable of breaking tolerance in MUC1.Tg mice. Plant Biotechnol J 9(9):991–1001. doi:10.1111/j.1467-7652.2011.00614.x

Ponndorf D, Ehmke S, Waliser B, Unger C, Görs S, Das G, Metges C, Broer I, Nausch H (2016) Production and stabilization of cyanophycinase in *Nicotiana benthamiana* and its functionality to hydrolyse cyanophycin in the murine intestine. Plant Biotechnol J (accepted). doi:10.1111/pbi.12658

Robert S, Khalf M, Goulet M-C, D'Aoust M-A, Sainsbury F, Michaud D (2013) Protection of recombinant mammalian antibodies from development-dependent proteolysis in leaves of *Nicotiana benthamiana*. PLoS One 8(7):e70203. doi:10.1371/journal.pone.0070203

Sainsbury F, Varennes-Jutras P, Goulet M-C, D'Aoust M-A, Michaud D (2013) Tomato cystatin SlCYS8 as a stabilizing fusion partner for human serpin expression in plants. Plant Biotechnol J 11(9):1058–1068. doi:10.1111/pbi.12098

Sallam A, Kalkandzhiev D, Steinbüchel A (2011) Production optimization of cyanophycinase ChpEal from *Pseudomonas alcaligenes* DIP1. AMB Express 1(1):1–9. doi:10.1186/2191-0855-1-38

Sallam A, Steinbuchel A (2010) Dipeptides in nutrition and therapy: cyanophycin-derived dipeptides as natural alternatives and their biotechnological production. Appl Microbiol Biotechnol 87(3):815–828. doi:10.1007/s00253-010-2641-0

Sallam A, Steinbüchel A (2009a) Process for the preparation of dipeptides from cyanophycin employing the isolated *Pseudomonas alcaligenes* DIP1 CGPase CphEal. Google Patents

Sallam A, Steinbuchel A (2009b) Cyanophycin-degrading bacteria in digestive tracts of mammals, birds and fish and consequences for possible applications of cyanophycin and its dipeptides in nutrition and therapy. J Appl Microbiol 107(2):474–484. doi:10.1111/j.1365-2672.2009.04221.x

Santi L, Batchelor L, Huang Z, Hjelm B, Kilbourne J, Arntzen CJ, Chen Q, Mason HS (2008) An efficient plant viral expression system generating orally immunogenic Norwalk virus-like particles. Vaccine 26(15):1846–1854. doi:10.1016/j.vaccine.2008.01.053

Santi L, Giritch A, Roy CJ, Marillonnet S, Klimyuk V, Gleba Y, Webb R, Arntzen CJ, Mason HS (2006) Protection conferred by recombinant *Yersinia pestis* antigens produced by a rapid and highly scalable plant expression system. Proc Natl Acad Sci U S A 103(4):861–866. doi:10.1073/pnas.0510014103

Santos S, Torcato I, Castanho MA (2012) Biomedical applications of dipeptides and tripeptides. Biopolymers 98(4):288–293

Solá RJ, Griebenow KAI (2009) Effects of glycosylation on the stability of protein pharmaceuticals. J Pharm Sci 98(4):1223–1245. doi:10.1002/jps.21504

Stevens LH, Stoopen GM, Elbers IJW, Molthoff JW, Bakker HAC, Lommen A, Bosch D, Jordi W (2000) Effect of climate conditions and plant developmental stage on the stability of antibodies expressed in transgenic tobacco. Plant Physiol 124(1):173–182. doi:10.1104/pp.124.1.173

Teh YHA, Kavanagh TA (2010) High-level expression of camelid nanobodies in *Nicotiana benthamiana*. Transgenic Res 19(4):575–586. doi:10.1007/s11248-009-9338-0

Terova G, Robaina L, Izquierdo M, Cattaneo A, Molinari S, Bernardini G, Saroglia M (2013) PepT1 mRNA expression levels in sea bream (*Sparus aurata*) fed different plant protein sources. SpringerPlus 2(1):17. doi:10.1186/2193-1801-2-17

Thomas DR, Walmsley AM (2014) The effect of the unfolded protein response on the production of recombinant proteins in plants. Plant Cell Rep 34(2):179–187. doi:10.1007/s00299-014-1680-x

Ufaz S, Galili G (2008) Improving the content of essential amino acids in crop plants: goals and opportunities. Plant Physiol 147(3):954–961. doi:10.1104/pp.108.118091

Webster DE, Wang L, Mulcair M, Ma C, Santi L, Mason HS, Wesselingh SL, Coppel RL (2009) Production and characterization of an orally immunogenic *Plasmodium* antigen in plants using a virus-based expression system. Plant Biotechnol J 7(9):846–855. doi:10.1111/j.1467-7652.2009.00447.x